

Influence of botanic origin and amylose content on the morphology of starch nanocrystals

Déborah LeCorre · Julien Bras · Alain Dufresne

Received: 24 June 2011 / Accepted: 4 November 2011 / Published online: 19 November 2011
© Springer Science+Business Media B.V. 2011

Abstract Starch nanocrystals (SNC) are crystalline platelets resulting from the disruption of the semi-crystalline structure of starch granules by the acid hydrolysis of amorphous parts. The aim of this study was to assess the influence of botanic origin and amylose content of native starches on the morphology and properties of resulting nanoparticles. SNC were prepared from five different starches normal maize, high amylose maize, waxy maize, potato, and wheat; covering three botanic origins, two crystalline types, and three range of amylose content (0, 25, and 70%) for maize starch. Different types of nanocrystals were obtained with a thickness ranging between 4 and 8 nm and diameter from about 50 to 120 nm depending on the source. The comparison of their morphology, crystallinity, and rheological properties is proposed for the first time. For the same amylose content, maize, potato, and wheat resulted in rather similar size and crystallinity of SNC proving the limited influence of the botanic origin. For the same botanic origin (maize), differences in size were more important indicating the influence of the amylopectin content. Also, particles tended to show square shapes with increasing native starch's amylopectin content and

A-type crystallinity. Thus, only high amylose content starches should be avoided to prepare SNC.

Keywords Starch · Nanocrystals · Botanic origin · Amylose · Hydrolysis · Rheology

Introduction

Polymers reinforced with nanosized particles, or nanocomposites are increasingly present in our society thanks to their unique properties at low filler content compared to conventional composites. Moreover, increasing environmental concerns have led to investigate the potential use of renewable resources to replace their non-renewable or fossil-based counterparts. Renewable resources, such as polysaccharides, present the added advantage to be available worldwide and from different plant sources limiting geopolitical conflicts. In the early 1990s, shortly after pioneer work on nanoclay-reinforced polymer nanocomposites by researchers at Toyota, work on cellulose nanofillers (such as whiskers) reinforced polymers started. Even if the number of studies on nanofibrillated cellulose has strongly increased last decade (Siró and Plackett 2010), most studies were carried out with cellulose nanocrystals (whiskers). They are obtained by the acidic elimination of the amorphous phase of cellulose; and a wide variety of plant source has been investigated showing a strong influence of botanic origin on their

D. LeCorre · J. Bras (✉) · A. Dufresne
LGP2, Laboratory of Pulp and Paper Sciences,
461, Rue de la Papeterie, BP 65, 38402 Saint Martin
d'Hères Cedex, France
e-mail: julien.bras@pagora.grenoble-inp.fr

morphological properties (Bras et al. 2011). It was soon followed by works on chitin and starch, mainly potato (Chen et al. 2008; Dufresne and Cavaille 1998) and waxy maize (Angellier 2005; Putaux et al. 2003) by extension. Most of the work consisted in determining the best hydrolysis conditions for a given polysaccharide and in checking reinforcement or barrier properties improvement of ensued nanocomposites.

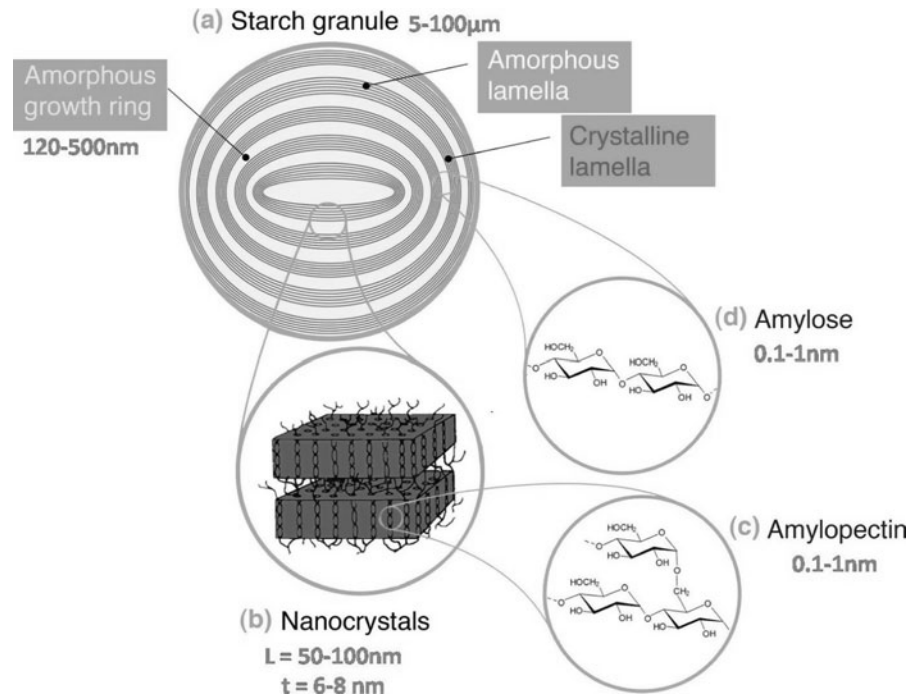
Starch is one of the most abundant biomass materials in nature and has already found numerous industrial applications. Carbohydrate chemists have developed numerous products that have greatly expanded starch use and utility (Whistler and BeMiller 2009). Indeed, acid hydrolysis has been used for a long time to modify starch and its properties. In industry, starch slurries are treated with dilute HCl or H₂SO₄ at 25–55 °C for various periods of time, to produce “acid-modified” starch used as sizing agents, in gum candies production, and in paper and paper board production. Most recent publications use either of these two acids for preparing starch nanocrystals (SNC), but conditions have been optimized over the years. In 1975, Battista reported the production of highly crystalline insoluble residues using HCl in 40 days (Battista 1975). In 1996, Dufresne et al. prepared so-called microcrystalline starch in only 15 days still using HCl (Dufresne et al. 1996). More recently (Angellier et al. 2004), the process for obtaining SNC was optimized, taking it down to 5 days using H₂SO₄. It was shown that the formation of sulfate-ester groups on the surface of the nanocrystals during H₂SO₄ hydrolysis limits the flocculation of the nanoparticles and leads to the production of more stable suspension (Angellier 2005). Even if the framework of this work is focused on SNC obtained by acid hydrolysis, it is possible, using other processes, to produce SNC as well as amorphous starch nanoparticles as recently described in a review on starch nanoparticles (Le Corre et al. 2010). Their use in polymeric matrices has also been recently detailed (Le Corre et al. 2010; Lin et al. 2011) and showed some important improvement of mechanical and barrier properties. Nowadays, the use of SNC is also being investigated for industrial packaging in a European research project (FlexPakRenew FP7 EU project). However, despite this increase of interest for the past 2 years, up to our knowledge, no studies have compared the influence of starch sources, considered what source can be used, and which will potentially

give the best nanocrystals with respect to their shape, size, and yield.

Depending on the botanic origin of starch, it is well known that native granules present a wide variety of size (2–100 μm), size distribution, shape, extraction from plant conversion factors, and chemical contents (Whistler et al. 1967). Starch granules consist of mainly two glucosidic macromolecules called amylose and amylopectin. Amylose is defined as a linear molecule of glucose units linked by (1–4) α-D-glycoside bonds, slightly branched by (1–6) α-linkages. Amylopectin is a highly branched polymer consisting of relatively short branches of α-D-(1-4) glycopyranose that are interlinked by α-D-(1-6)-glycosidic linkages approximately every 22 glucose units (Dufresne 2007). The predominant model for starch structure is multi-scaled and consists in the granule (2–100 μm), into which are found growth rings (120–500 nm) composed of blocklets (20–50 nm) made of amorphous and crystalline lamellae (9 nm, Gallant et al. 1997) containing amylopectin and amylose chains (0.1–1 nm) as represented in Fig. 1. Native starches contain between 15 and 45% of crystalline material. It is believed that the crystalline region is created by the intertwining of chains with a linear chain length above 10 glucose units, to form double helices (Oates 1997) which are packed and form the crystallites; and the amorphous region corresponds to branching points. Amylose molecules are thought to occur in the granule as individual molecules, randomly interspersed among amylopectin molecules and in close proximity with one another, in both the crystalline and amorphous regions (Oates 1997). Depending on the botanic origin of starch, amylose is preferably found in the amorphous region (e.g., wheat starch), interspersed among amylopectin clusters in both the amorphous and crystalline regions (e.g., normal maize starch), in bundles between amylopectin clusters, or co-crystallized with amylopectin (e.g., potato starch). Amylose content and botanic origin should therefore considerably influence the crystalline organization.

Depending on their X-ray diffraction pattern, starches are categorized in three crystalline types called A, B, and C. Imberty et al. (Imberty et al. 1987; Imberty and Perez 1988) proposed a model for the double helices packing configuration to explain difference between A- and B-type starches. A-type structures are closely packed with water molecules

Fig. 1 Representation of the starch granule multi-scale structure adapted from Le Corre et al. (2010)



between each double helical structure, whereas B type are more open and water molecules are located in the central cavity formed by six double helices as shown in Fig. 2.

This difference in crystalline types could render different nanocrystals morphology. However, this point has never been investigated. The aim of this study is to assess the influence of some botanic origin, amylose content, and crystalline type of native starches on the features and properties of resulting SNC.

Experimental

Materials

Starches were kindly provided by Cargill (Krefeld, Germany) according to requirements: waxy maize starch (C* Gel 04201, 98% amylopectin), normal maize starch (Cerestar RG 03453), amylo maize (Amylogel 03003, 65–75% amylose), potato starch (C* Gel 30002), and wheat starch (Cerestar PT 20002). Sulfuric acid (96–99%, Sigma Aldrich) was used after dilution at 3.16 M with distilled water. Pure amylose from potatoes (10130, Fluka) and pure amylopectin from potato starch (10118, Sigma) were used as references in the iodine-binding test.

Preparation of starch nanocrystals

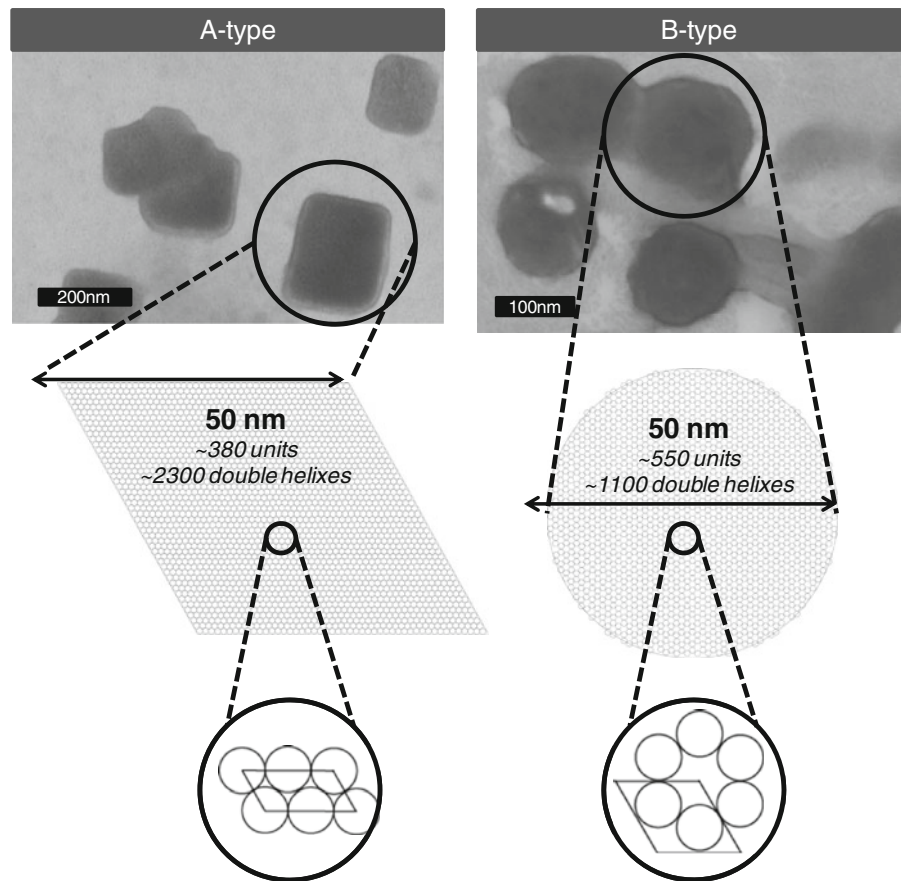
The optimized hydrolysis process developed by Angellier et al. (2004) was adapted to 1 L to prepare nanocrystals from the five different starches. Briefly, 147 g of native starch was mixed with 1 L of previously prepared diluted sulfuric acid (3.16 M). The suspension was kept under 100 rpm mechanical stirring at 40 °C, using a silicon bath, for 5 days. The final suspensions were washed by successive centrifugation with distilled water until reaching neutral pH and re-dispersed using Ultra Turrax for 5 min at 13,000 rpm to break aggregates. The obtained suspensions were filtered on a filter tissue (40 μm, ref. 03-41/31 Buisine, France). Sodium azide was added to the suspensions before storage at 4 °C to avoid microbial growth.

Starch nanocrystals characterization

Microscopies

An environmental scanning electron microscope (ESEM) on a Quanta 200 FEI device (Everhart–Thornley Detector) was used at high voltage (10 kV) to confirm the morphology of native starches. Native starches were simply deposited onto carbon tape before observation.

Fig. 2 Double helices packing configuration depending on crystalline type and corresponding picture of starch nanocrystals from waxy maize starch (*A-type*) and high amylose starch (*B-type*)



The morphology and average dimensions of SNC were studied using a Zeiss Ultra 55 Field Emission Gun Scanning Electron Microscope (SEM/FEG) equipped with a STEM detector. All samples were prepared by depositing 2.5 μL of SNC suspension (with concentration 0.01 wt%) on a TEM grid. A thin Au–Pd conductive coating (ab. 1 nm) was deposited on top of the sample to reduce charge effect. The best compromise in terms of SNC contrast and residual charge was obtained at 10 kV accelerating voltage and working distance of about 6 mm. In order to obtain the best possible resolution, the secondary electron imaging mode with the In-lens detector was preferred (reflective mode). However, some samples were better observed in the transmission mode using the STEM detector. The average dimensions were determined using digital image analyses. Starch nanoparticles were assimilated to spherical particles. Between 70 and 500 measurements were performed depending on the source to determine the average diameter and standard deviation.

Atomic force microscopy (AFM) measurements were performed on a Multimodal AFM (DI, Veeco, Instrumentation Group) with both tapping and conductive mode (C-AFM). The tips were Multi130 for tapping and MESP for C-AFM. A drop of a SNC suspension was deposited on a mica substrate (split with adhesive tape) and dried for a few minutes at 40 °C. Between 30 and 110 measurements were performed depending on the source to determine the average thickness and standard deviation.

Determination of amylose/amylopectin ratio by iodine-binding capacity

This procedure consists in staining a dilute suspension of starch with potassium iodine/iodine solution ($\text{KI}:\text{I}_2$) and analyzing the absorbency of the suspension. To determine the amylose content, a solution of potassium iodine and iodine with $\text{KI}:\text{I}_2$ 10:1 was prepared according to Williams et al. (1970) and added to the diluted starch suspension. The absorbencies of the

iodine stained solutions were measured using a UV–VIS spectrophotometer (Unicam UV5 Serie, Thermo Spectronic, Cambridge, UK) at 650 nm for amylose and at 540 nm for amylopectin, their respective absorbance maxima (Shannon et al. 2009). A correlation between absorbance at 600 nm and amylose content according to a rapid single-wave colorimetric method (McGrance et al. 1998) was assessed. The equation modeling this relationship allows us to determine the amylose content of some SNC.

X-ray diffraction

Wide angle X-ray diffraction analysis was performed on powder obtained from both native starch and air-dried SNC suspensions kept at ambient temperature (23 °C) and relative humidity (28.8%). The samples were placed in a 2.5-mm deep cell and measurements were performed with a PANanalytical, X'Pert PRO MPD diffractometer equipped with a X'celerator detector. The operating conditions for the refractometer were Cu K_{α} radiation, 2θ between 4 and 44°, step size 0.067°, and counting time 90 s.

The degree of crystallinity of the samples was quantitatively estimated following the method of Nara and Komiya (1983) adapted, also called the “two-phase” method. A curve connecting the peaks baseline was plotted on the diffractogram. The area above the curve was assumed to correspond to the crystalline domains, and the lower area to the amorphous part. The ratio of upper area to total area was taken as the degree of crystallinity.

However, Lopez-Rubio et al. reported that this “two-phase” method may underestimate the crystalline content of starches as it does not take into account the diffuse scattering from non-perfect crystalline

structures (Lopez-Rubio et al. 2008). Therefore, a second set of measurements, using more complete statistical method of analysis, was performed. Samples were conditioned at 90% RH as higher water content increases the definition of crystalline peaks. Indeed, the chiral side-chain liquid–crystalline model for starch proposed by Waigh et al. considers that an amylopectin molecule consists of three sections: the chiral double helices, the amorphous spacers, and the amorphous backbone (Waigh et al. 2000a). It is postulated that the crystalline smectic lamellar periodicity is due to the antagonistic effect of the entropy of the backbone and the ordering of the helices. The entropy gain of the side chains and the backbone on plasticization by the water molecules pushes the helices into a lamellar structure due to the reduced free energy of this configuration (Waigh et al. 2000b).

Rheological measurements

Rheological measurements were carried out using a controlled stress rheometer (MCR 301, Anton Paar Physica, Austria) calibrated and certificated, with a cone-plate fixture at 25 °C controlled via a Peltier system, and a solvent trap was used to prevent solvent evaporation.

Results and discussion

Preparation of starch nanocrystals

In order to investigate a wide range of structural differences, the following criteria were chosen to select starches amylose content, crystalline type, size of the native granules, and botanic origin. Some

Table 1 Main features of selected starches

Botanic origin	Granular size (μm)	Amylose (%) ^a	Non glucosic material (%)			Crystalline type	Referred to as
			Lipids ^b	Proteins ^b	Ash ^b		
High amylose	5–20	65–75	1.11	0.50	0.20	B	M70
Normal maize	5–20	27	0.61–0.65	0.30	0.10	A	M27
Waxy maize	5–20	1	0.23	0.10	0.10	A	M1
Wheat	2–30	28	0.24	0.33	0.30	A	W28
Potato	5–80	21	0.09	0.05	0.30	B	P21

^a Supplier data

^b Duprat et al. (1980). % of dry starch

criteria like amylose content and crystalline types can be linked for maize starch (Cheatham and Tao 1998). It also seems obvious when analyzing starch and starch nanocrystals' structure as detailed in Fig. 1.

Therefore, three types of maize starches covering a wide range of amylose content were selected (Table 1) waxy maize, normal maize, and high amylose maize starches. Potato starch presenting B-type crystallinity, a bimodal granular size distribution and particularly large granules was also selected. We also used wheat starch that presents a multi-modal granular size distribution with larger A-type granules and possibly smaller B-type ones.

The crystalline type could indeed have its importance. Imberty et al. proposed a model for the double helices packing configuration to explain the difference between A- and B-types starches (Imberty et al. 1987; Imberty and Perez 1988). A-type structure is closely packed with water molecules between each double helical structure, whereas B-type is more open with water molecules being located in the central cavity formed by six double helices as shown in Fig. 2. It was later envisaged that branching patterns of the different types of starch may also differ (Jane et al. 1997). C-type starch pattern has been considered to be a mixture of both A- and B-types since its X-ray diffraction pattern can be resolved as a combination of the previous two.

The five selected starches were treated following the 5-day optimized acid hydrolysis process (Angellier et al. 2004) in order to obtain SNC. Ensuing nanoparticles were labeled according to their botanic source

(M for maize, W for wheat, and P for potato) and amylose content. For instance, sample M27 refers to maize starch with 27% amylose. All preparations were successful and their features are gathered in Table 2.

Influence of botanic source on crystallinity

This part of the investigation aimed at checking if the acid hydrolysis treatment effectively led to the removal of amorphous domains of starch granules while leaving the crystalline part intact regardless the botanic source and amylose content. The degree of crystallinity of starch samples before and after hydrolysis was calculated following two methods as explained in the “Experimental” section. The first method (“two-phase” method) performed at ambient temperature and relative humidity is based on the ratio of the area of crystalline peaks to the total area of the diffractograms. Results are reported in Table 2 for native starch granules and SNC from the five different sources. The second method performed at 90% RH took into account diffuse scattering from non-perfect crystalline structures. This second set of measurements uses a more complete statistical method of analysis (not presented here). For all samples, it was observed that the degree of crystallinity was underestimated by 10% in average when using the “two-phase” method. As expected, the acid hydrolysis treatment induces an increase of the degree of crystallinity of the material (Table 2).

Figure 3 shows the diffraction patterns obtained for A-type maize starch (M27) (panels a and b) and B-type

Table 2 SNC features and influence of hydrolysis on crystallinity

Starch type	Crystallinity (%)			Amylose (%)	Diameter		Thickness		Percolation (%)		
	Native	SNC	ΔC		nm	Counts	nm	Counts	Celzard et al. (1996)		Lu and Mai (2005)
									Inf	Sup	
M70	23	35	12	11	118 ± 53	190	7.6 ± 1.6 ^a	76	7.1	10.8	13.9
M27	28	42	14	1	58 ± 36	576	6.1 ± 1.9 ^a	112	11.4	17.1	22.7
M1	34	48	14	0	47 ± 42	71	5 ± 1.6 ^b	14	11.5	17.3	22.9
W28	25	35	10	NA	100 ± 50	71	8.3 ± 3.1 ^c	30	9.1	13.8	17.9
P21	28	43	15	0	52 ± 4	951	3.7 ± 0.6 ^a	31	7.8	11.9	15.3

NA non available

^a Personal measurements using Gwyddon

^b Conducted at SMPC, Mons, Belgium

^c Personal measurements on AFM software

high amylose starch (M70) (panels c and d). The diffractograms obtained for both the native granules (panels a and c) and hydrolyzed granules (panels b and d) are reported. The relative area of crystalline peaks (e.g., 28 and 23% for native M27 and M70, respectively) is clearly increased after acid hydrolysis (42 and 35% for SNC obtained from M27 and M70, respectively) proving an increase in crystallinity. Values obtained for native starches are somewhat comparable to that found in the literature (Cheetham and Tao 1998; Lopez-Rubio et al. 2008) and no significant difference between A- and B-type was observed. The extent of the increase of the degree of crystallinity on acid hydrolysis (ΔC) is reported in Table 2 and similar values were observed for both sources of starch. However, the degree of crystallinity remains low even after acid hydrolysis showing that an important amount of non-organized materials remains in the SNC suspension.

As described earlier, the crystallinity of starch is attributed to the packing of double helixes formed by amylopectin side chains (Fig. 1). Therefore, amylopectin-rich starches are more crystalline than amylose-rich ones (e.g., M1 vs. M70, Table 2) (Cheetham and Tao 1998). It can be seen when plotting the evolution of the degree of crystallinity as a function of amylose content for native starch granule from the same botanic origin (Fig. 4a). However, the increase in crystallinity remains quite low compared to the increase in amylopectin content. An important amount of amylopectin chains remains in a non-organized state.

Higher crystallinity was expected for hydrolyzed amylopectin-rich (waxy) starch since there is less amorphous starch to hydrolyze. Indeed, when looking at the evolution of the degree of crystallinity of SNC as a function of increasing amylose content of native starch (Fig. 4a), a decrease is observed. Therefore, it seems that the higher the crystallinity of native starch, the higher the crystallinity of the ensuing SNC. The two curves corresponding to native starch granules and SNC are simply vertically shifted even if increased differences were expected for high amylopectin contents. Indeed, for starches with already relatively high crystallinity, the relative gain in crystallinity was limited.

However, two important parameters should be taken into account when interpreting the data. The first one is related to acid hydrolysis conditions we

used, as they were optimized for waxy maize starch. It is probable that optimized conditions should be different for other botanic sources. The second parameter which is interconnected with the first one is that more crystalline domains in amylopectin-rich starch should be more easily accessible for acid hydrolysis. It might, with this long process, hydrolyze defective crystallites and induces solubilization of part of the crystalline structure.

For starches with similar amylose content but from different botanic origin, no significant differences were observed for the degree of crystallinity of both native granules and SNC (Fig. 4b). The crystalline type does not seem to play an important role (comparing potato and normal maize), nor only the botanic origin (comparing normal maize and wheat). Consequently, the most important parameter determining the degree of crystallinity of SNC seems to be the amylopectin content.

Influence of botanic source on amylose content of starch nanocrystals

As already explained and described in Fig. 1, SNC are thought to consist in amylopectin side chains (Robin 1976). To verify the accuracy of this assumption, the amylose/amylopectin ratio needs to be assessed for all starches before and after hydrolysis. There are a lot of different techniques for determining the amylose content in starches. The most readily used is iodine binding. It exploits the ability of iodine to stain amylose and amylopectin helixes by forming amylose-iodine complexes. Although potentiometric titration offers the most definitive measurement of the iodine-binding capacity of a sample, spectrophotometric determinations are more widely used because of convenience and simplicity of use (Knutson 2000).

The use of this method for native starches confirmed differences in initial amylose content. However, suspensions made of freeze-dried starch re-dispersed in water colored very slightly in excess iodine but did not stain.

Bailey and Whelan reported that when hydrolyzed (i.e., decreasing chain length) in random fashion by acid or alpha-amylase both polysaccharides gradually lose the capacity to stain with iodine (Bailey and Whelan 1961). The blue amylose color becomes purple, then red, brown, and finally disappears. The blue color for the stain is due to the amylose

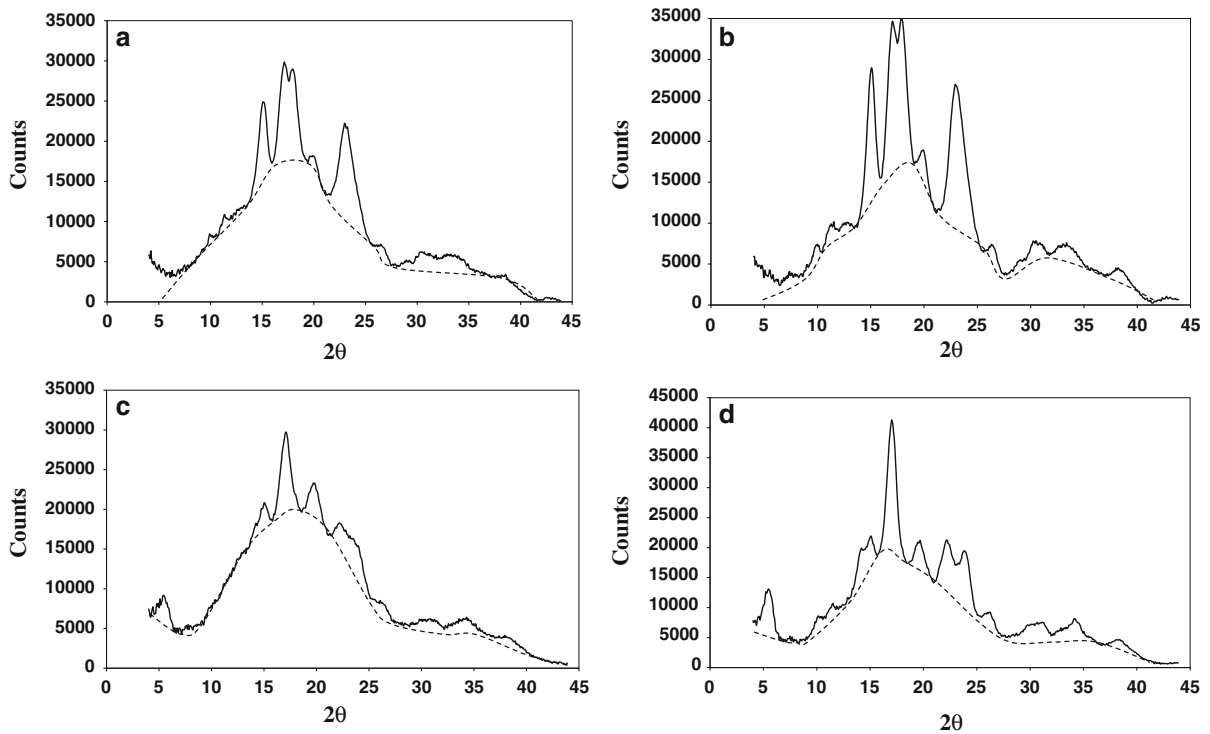


Fig. 3 A-type maize starch X-ray diffraction patterns for **a** native starch and **b** starch nanocrystals and B-type high amylose maize starch X-ray diffraction patterns for **c** native

starch, and **d** starch nanocrystals. The *dashed line* is a schematic representation of the limit between crystalline peaks and the amorphous part

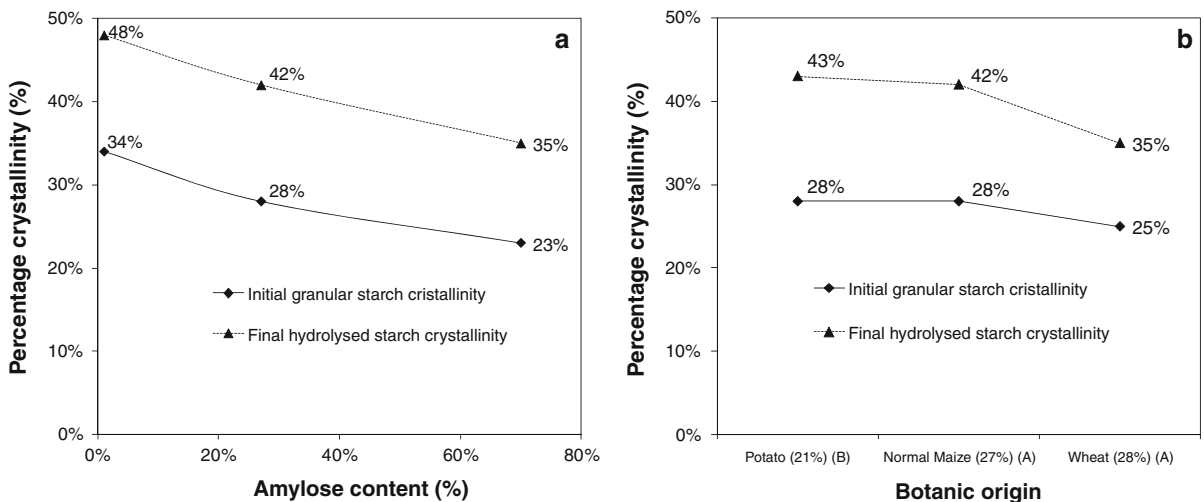


Fig. 4 Original crystallinity (*filled diamond*) and final crystallinity (*filled triangle*) for starches with same amylose content and different botanic origin (**a**) and for starches with same botanic origin and different amylose content (**b**)

component of starch. The amylopectin gives a red–purple color which is less intense than the amylose stain. Indeed, for amylose–iodine helical inclusion

complex to form, the chains have to be at least 18 unit long. The amylopectin double helical structure has been reported to consist of about 15 glycosyl units

[DP = 15 close to 5.3 nm in length for potato (Robin 1976), DP = 14.2 close to 5 nm in length for waxy maize (Angellier-Coussy et al. 2009)] and the amylose is quickly depolymerized during hydrolysis, which could explain why no lasting coloration was observed for SNC samples. This consideration rules out all techniques consisting in complexing amylose with another reagent for determining its content in SNC.

However, this non-coloration could also reveal that freeze-drying affects the complexing properties of hydrolyzed starch. It might, for instance, favor double helixes formation stabilized by hydrogen bonding during the slow drying, and prevent solubilization and complex inclusion with iodine.

As the same reagent for dissolving starch was used to prepare the native starch and SNC suspension before testing, tests were duplicated without the treatment. This treatment was suspected to further de-polymerize residual chains. However, results were similar than without pre-treatment.

Further tests were carried out for never-freeze-dried maize SNC suspensions. They exhibited different colorations ranging from light brown to yellow for high amylose content starch to waxy maize, respectively. Indeed, UV–VIS absorption spectra for SNC suspensions clearly differed from that of their native counter parts, whereas they were closer to the pure amylopectin reference as presented in Fig. 5. Maximum absorption for amylose–iodine complex is around 630 nm. Native starches exhibit a peak around 600 nm. All SNC suspensions showed maximum absorption around 400 nm (magenta) which reflects

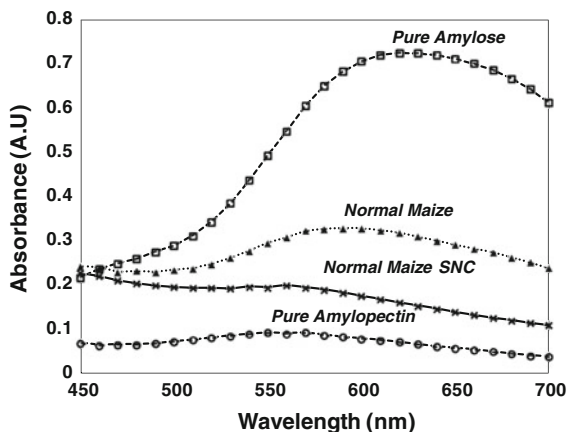


Fig. 5 Absorption spectra of normal maize starch nanocrystals with native, amylose, and amylopectin references

the yellowish color of the samples due to iodine. For clarity, this wavelength is not presented in Fig. 5. High amylose and normal maize SNC suspension also exhibit a large peak around 560 nm (green) representative of their brownish-purplish color. This wavelength is supposed to be the maximum absorption for amylopectin–iodine complex. Waxy maize nanocrystals suspension did not stain. No peak was observed at higher amylose–iodine complex absorption wavelength for SNC. Figure 6 shows the correlation between absorbance at 600 nm and amylose content according to a rapid single-wave colorimetric method (McGrance et al. 1998). The equation modeling this relationship allows us to determine that the amylose content of P21, M1, M27, and M70 is, respectively, 0%, 0% (or too low a DP to be measured), 1% ± 1.8% and 11% ± 2.1% (as reported in Table 2, Fig. 6). Results suggest that SNC suspensions are mainly made of low DP amylopectin.

Given the uniqueness of the samples, authors will dedicate another study to the assessment of quantitative amylose/amylopectin content in SNC.

Influence of botanic source on starch nanocrystal morphology

Figures 7, 8, and 9 show SEM images obtained for native starch granules and their corresponding SNC with different botanic origins (Fig. 7), amylose contents (Fig. 8), and crystalline types (Fig. 9). As for

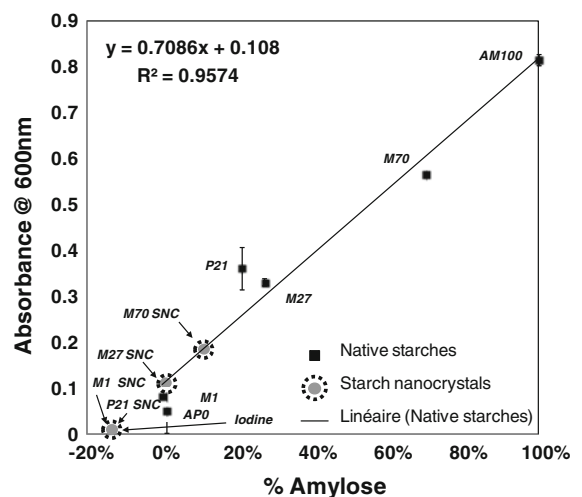


Fig. 6 Calibration graph of absorbance at 600 nm against percentage amylose for native starches (McGrance et al. 1998)

native granules, SNC display very different shapes, size, and size distribution.

Regarding the shape of the nanoparticles, no correlation with botanic origin (Fig. 7) or amylose content (Fig. 8) was observed. Their morphology seems to be mainly linked to the crystalline type (Fig. 9). Indeed, waxy maize and wheat starch (A-type) rendered, respectively, parallelepipedic and square-like nanocrystals. Nanocrystals obtained from normal maize starch were more difficult to characterize since no precise shapes were recognized. High amylose maize SNC (B-type) were rather round and potato SNC (B-type) seemed to be made of both round and rounded-corner-square particles depending on size. Hence, schematically nanocrystals produced from A-type starches rendered square-like particles, whereas nanocrystals produced from B-type starches

rendered round-like particles. This could be explained by the different packing configurations of amylopectin chains for A and B-type starches as shown in Fig. 2. The A-type closely packed configuration displays a parallelepipedic pattern, whereas the B-type cavity-like configuration displays a circular one. The packing of these patterns might render, respectively, square-like and disk-like particles. These results prove for the first time the importance of starch crystalline type on nanocrystals shape. It should also be considered that the SNC observed might correspond to the crystalline part of the blocklets reported by some authors thus explaining the size distribution among SNC.

Starch nanocrystals' size and size distributions were assessed by SEMFEG image analysis. Results are reported in Fig. 10. For a given botanic origin (i.e., maize starch, Fig. 10a), a sliding of size distribution's

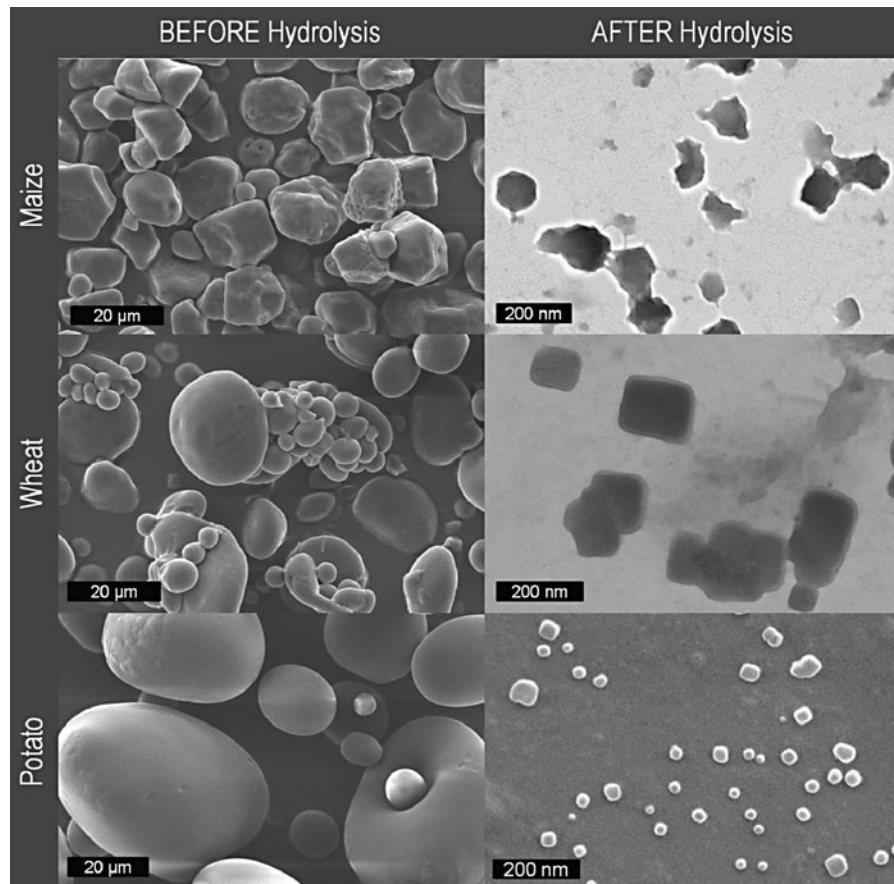


Fig. 7 Scanning electron microscopy micrograph of starches before (*first column*) and after (*second column*) hydrolysis for different botanic source

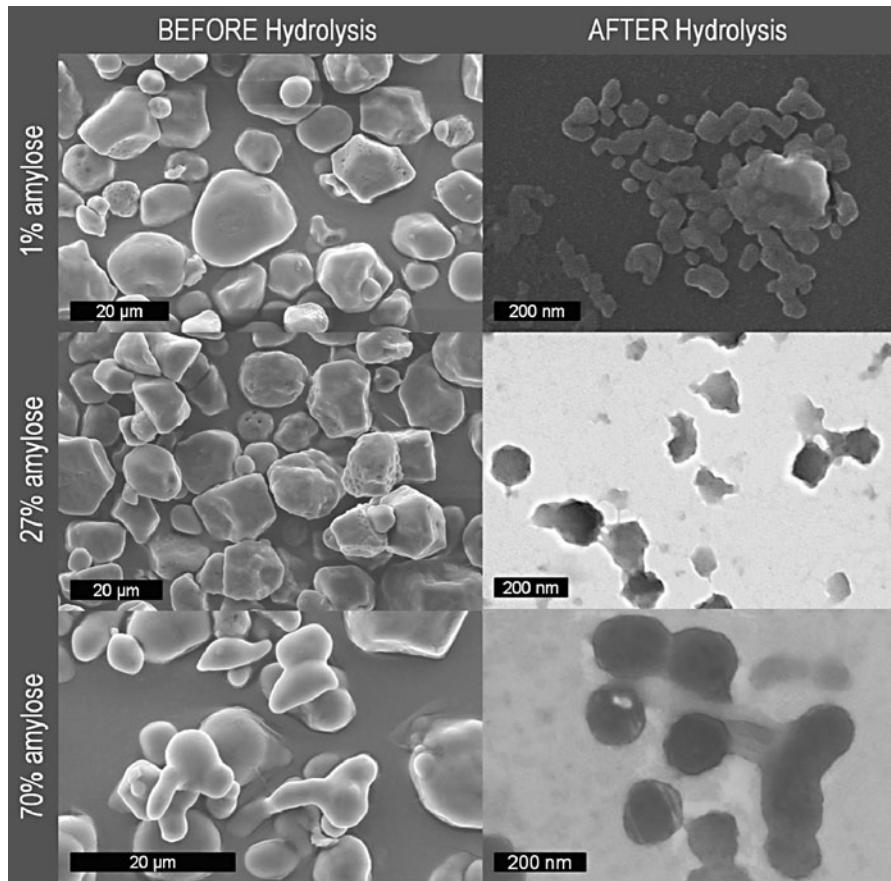


Fig. 8 Scanning electron microscopy micrograph of maize starch before (*first column*) and after (*second column*) hydrolysis for increasing amylose contents. The lower the amylose content, the squarer the final particles

main peak is observed with increasing the amylose content. This result is not surprising since amylose is believed to jam the pathways for hydrolysis. It makes it slower, harder and renders, for a given time, bigger particles (or aggregates) when amylose content is high.

Differences in size and size distribution were also observed for starches from different botanic origin with similar amylose content as shown in Fig. 10b. No tendency linked neither to the degree of crystallinity nor to the crystalline type was observed for nanocrystals sizes since

- (i) for the same amylose content wheat starch nanoparticles (W28) are almost twice as big as normal maize SNC (M27), and
- (ii) for the two different crystalline types (A and B) corresponding to normal maize starch (M27) and

potato starch (P21), respectively, SNC have almost the same size.

However, as mentioned before, it has been reported that depending on the botanic origin of starch, amylose is preferably found in the amorphous region (Blanshard 1987) (e.g., wheat starch), or interspersed among amylopectin clusters in both the amorphous and crystalline regions (e.g., normal maize starch) (Kasemsuwan and Jane 1994), or in bundles between amylopectin clusters, or co-crystallized with amylopectin (e.g., potato starch) (Blanshard 1987). It most likely influences the hydrolysis patterns of starches. Also, some authors reported different size of blocklets depending on the botanic origin of starch. Long axial diameters of the blocklets are 10–30 nm for maize starches (Baker et al. 2001), 20–50 nm for potato starches (Szymonska and Krok 2003), and 25–100 nm

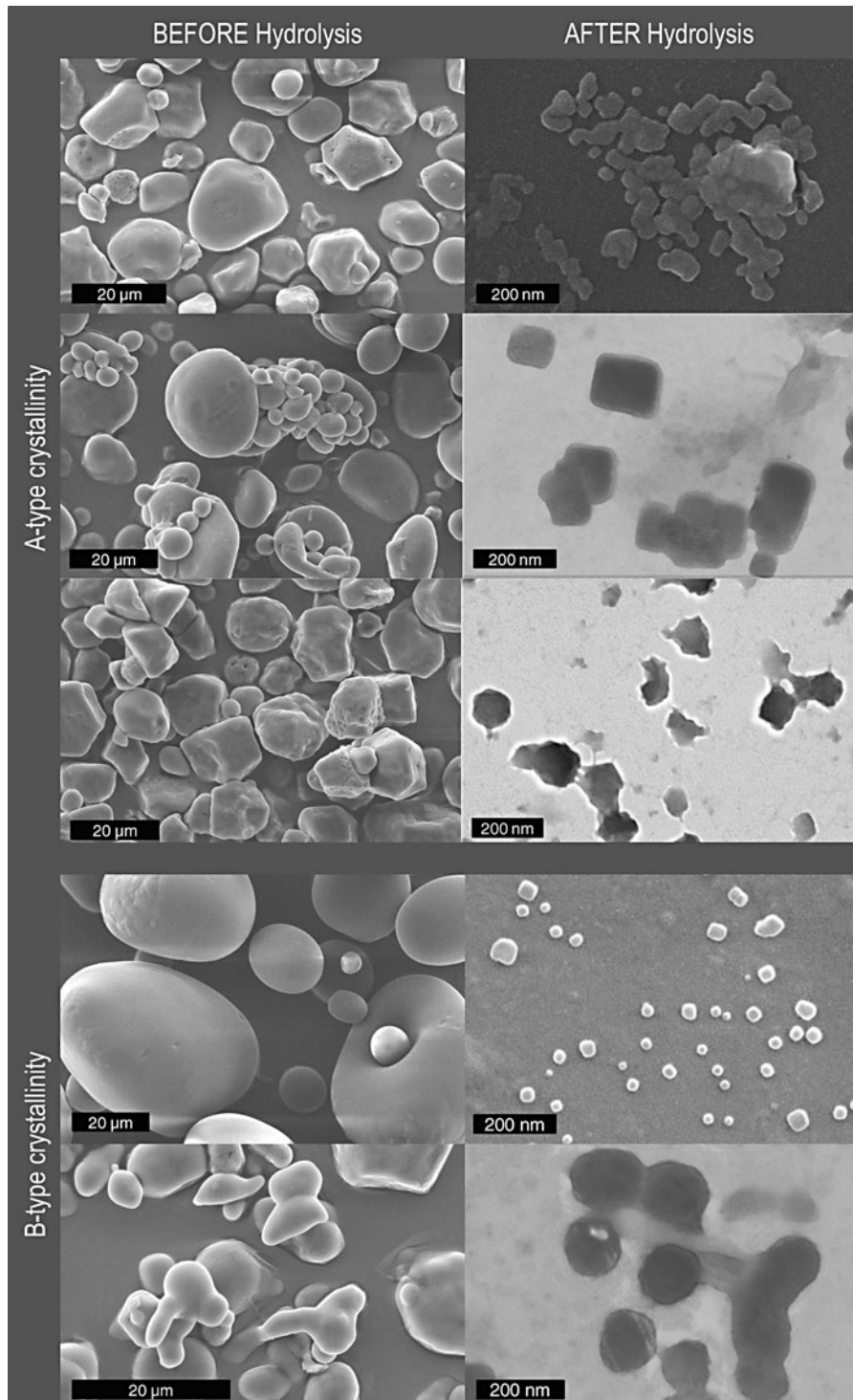


Fig. 9 Scanning electron microscopy micrograph of starches before (*first column*) and after (*second column*) hydrolysis for different crystalline types

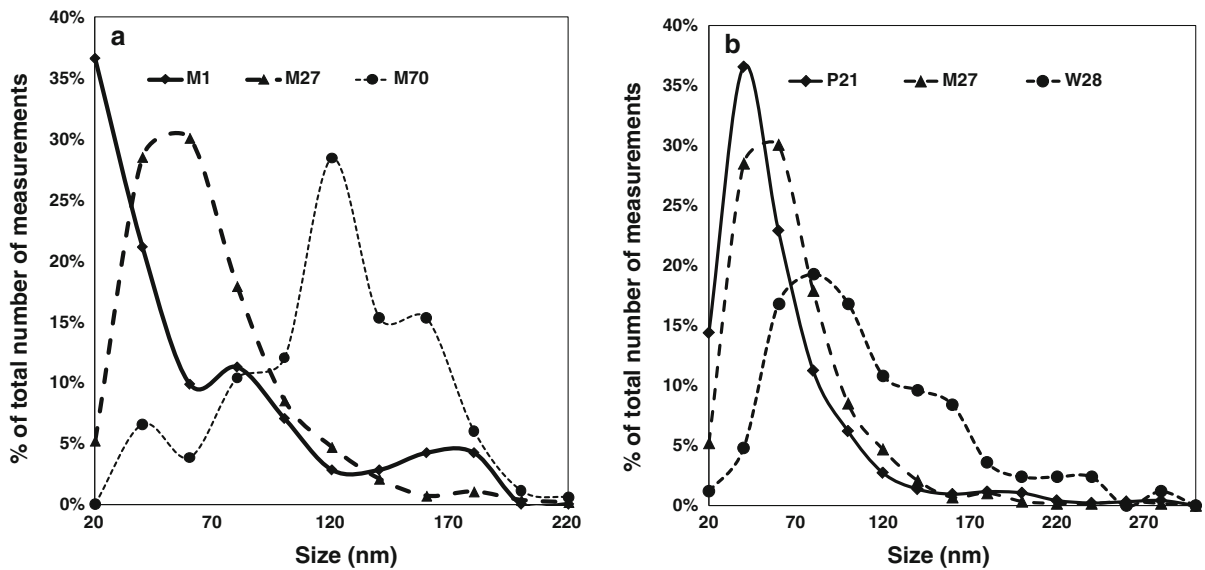


Fig. 10 Size distribution for **a** the same botanic origin and **b** the same amylose content

for wheat starches (Perez et al. 2009) thus giving a possible explanation for bigger wheat SNC.

Influence of botanic source on starch nanocrystal thickness

As mentioned earlier, SNC are described as platelets resulting from the hydrolysis of branching point (amorphous lamellae) of the alternating crystalline lamellae associated with crystallites made of packed amylopectin double helices. To confirm and assess the thickness of those platelets, AFM measurements were carried out on the different SNC.

Measured thicknesses were between 4 and 8 nm and values are reported in Table 2. Our results seem to be in accordance with current models (Angellier-Coussy et al. 2009; Gallant et al. 1997; Robin 1976) which report the crystalline lamellae to be 5–7 nm and the cumulated size of crystalline and amorphous lamella to be 9–10 nm for all starches (Gallant et al. 1997). Thus, this confirms that SNC are individualized crystallites. Also, it is suggested in literature (Gérard et al. 2000; Jane et al. 1997) that the B-type amylopectin branching points are clustered in an ensued smaller amorphous lamella (i.e., thicker crystalline lamellae), whereas A-type amylopectin branching points are scattered in both the amorphous and the crystalline regions, giving more flexibility (lower entropy barrier) to double helices for packing

closely (i.e., thinner crystalline lamellae). Unfortunately, the use of different software for the measurements analysis makes it difficult to compare the values and their accuracy. Nevertheless, as expected, high amylose (B-type) SNC were thicker than normal maize SNC, itself thicker than waxy maize SNC. However, no relationship to amylose content (%) can be postulated. Indeed, for the same amylose content, wheat SNC were much thicker than others, and surprisingly potato SNC were significantly thinner and better individualized than any other nanocrystals. This last phenomenon might be explained by the use of ultrasonic treatment but also by the different locations of amylose inside the granules. Thus, it seems that the thickness of SNC is rather linked to the botanic origin of starch via its internal organization (i.e., where the amylose is located inside the granule) as explained in the “Influence of botanic source on starch nanocrystal morphology” section.

Viscosity of starch nanocrystal suspensions

The ultimate objective of the project (FlexPakRenew FP7 EU project) within which this study was undertaken aims at using SNC for the development of complex flexible packaging. The rheological behavior of SNC aqueous suspensions is therefore important for the processing of such materials. The type of information sought for was twofold:

1. get useful information for the processing of such suspensions, and
2. determine experimentally the percolation threshold of the suspensions.

First, waxy maize SNC suspensions were prepared at different concentrations. All suspensions display a shear-thinning behavior as presented in Fig. 11 and fit a power-law distribution. Indeed, a fitting with Heschel–Buckley's model rendered a yield stress (τ_0) equal to zero. The flow behavior index, n , varies only moderately with increasing the SNC content suggesting that we remain far from the percolation threshold.

Previous work (Araki et al. 1999) has shown the influence of surface charge on cellulose nanocrystals and demonstrated that nanocrystals produced by sulfuric acid hydrolysis presented surface charges which limited time dependency. As their cellulosic counter parts, SNC suspensions showed little time dependence at low shear rate (stable measurements, results not presented) and measurements were reproducible as the error bars in Fig. 11 are smaller than the size of symbols.

The suspensions' viscosity displayed moderate power-law-concentration dependence which increased with decreasing shear rate. On industrial machines, a SNC suspension will undergo very high shear during very little time. For example, on a coating machine shear rate will be about 10^5 s^{-1} for a couple of milliseconds. At such shear rate, the suspension will be damaged and particles might artificially aggregate. Therefore, there is no point in studying its behavior with a time ramp at high shear rate. On the contrary, to

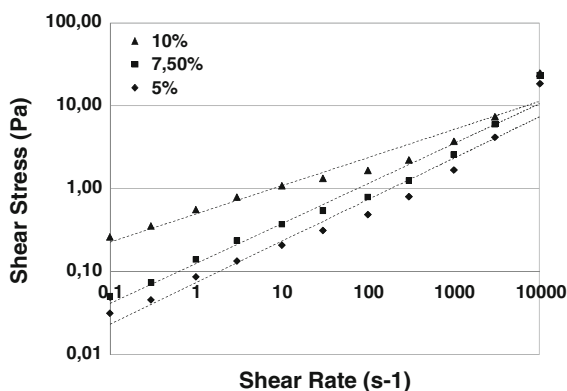


Fig. 11 Waxy maize starch nanocrystals suspension power-law fitting and corresponding Heschel–Buckley's coefficients

work with stable SNC suspensions, studies at relatively low shear rate and longer time will be preferred. This is why the different SNC suspensions have been studied at 10 s^{-1} after 60 s stabilization. Suspensions with different SNC concentrations have been prepared for each source of starch and results are shown in Fig. 12.

No particular relationship was found between viscosity and SNC size, thickness, surface area, or specific surface. However, suspensions with lowest viscosity were M70 and P21 which corresponds to suspensions with, respectively, disc-like morphology and ill-defined morphology (mix of square and disc) nanoparticles. Highest viscosity was achieved with wheat starch (W28) which presents square-like platelets SNC.

Flow properties of SNC suspensions have been studied for different concentration seeking the rheological percolation concentration. Unfortunately, above 15 wt% SNC suspensions formed “cakes” in the gap of the cone-plane rheometer preventing from measuring the sought data. In previous papers (Dufresne and Cavaillé 1998; Celzard et al. 1996), the percolation threshold for SNC in a polymeric matrix were determined using water uptake measurements. They were reported to be 20 vol% (31 wt%) and 6.7 vol% (10 wt%), respectively, for potato SNC (Dufresne and Cavaillé 1998) and waxy maize SNC (Angellier et al. 2005) thus explaining why no percolation threshold was observed during our rheological measurements (limited to 10 wt%).

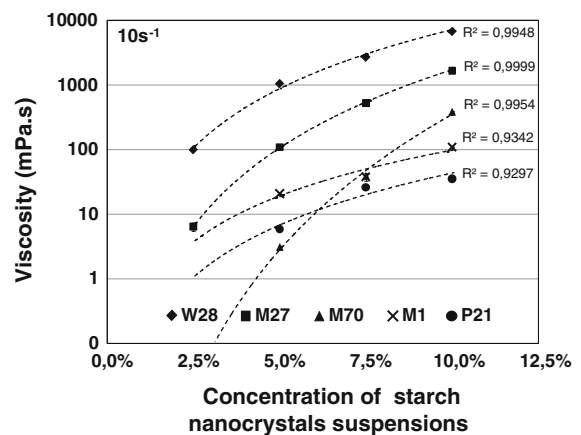


Fig. 12 Evolution of viscosity of starch nanocrystal suspensions with increasing concentration at 10 s^{-1} . Dashed lines are power-law fittings

Models for calculating the percolation threshold of clay nanoparticles can be found in the literature. Celzard et al. proposed the “excluded volume model,” from which Eq. 1 was extracted, to assess the percolation threshold of high aspect ratio nanoclay (Celzard et al. 1996). Lu and Mai determined recently Eq. 2 using a re-normalization group approach for characterizing the barrier properties of nanoclay (Lu and Mai 2005).

$$1 - \exp\left(-\frac{3.6t}{\Pi d}\right) \leq \phi_c \leq 1 - \exp\left(-\frac{5.6t}{\Pi d}\right) \quad (1)$$

$$\phi_c = \frac{2.154t}{d} \quad (2)$$

within both equations d the diameter and t the thickness of the particles. According to Li et al. these two models underestimate the percolation threshold (Li and Kim 2007). Table 2 shows the theoretical percolation threshold for each botanic source according to each model.

Differences are observed for the different botanic sources regardless the model. Indeed, both high amylose maize (M70) and potato (P21) SNC display the lowest percolation thresholds. Unfortunately, such differences are not observed in our viscosity measurements and do not seem to be related to amylose content. This might either be due to the fact that our viscosity measurements are at too high a shear rate, or to the polydispersity of SNC in suspensions. Nevertheless, one could notice that these two types of SNC were prepared from B-type starches, and both render more or less disc-like nanoparticles. However, the data from the models are in contradiction with previously reported values according to which potato SNC's percolation threshold (31 wt%) is higher than that of waxy maize SNC (10 wt%), as mentioned earlier.

Therefore, concerning coating applications, no starch source is preferred even though waxy maize SNC seems to be the best compromise with rather low viscosity and small square-like shaped nanocrystals.

Conclusion

It has always been suspected that the type of starch used for producing SNC was an important parameter. This study shows for the first time that the botanic origin of starch shows only a moderate influence (through the distribution of amylose inside the granule and blocklet

size) on final properties of ensuing SNC (such as size, size distribution, thickness, and viscosity), whereas amylose content and crystalline type would be more of influence (on, respectively, size and shape). Differences in size are rather moderate, whereas differences are more pronounced when comparing shapes and crystallinity. In the intent to use SNC as filler in polymeric matrices, more attention should be brought to selecting the native starch. Indeed, when seeking for barrier properties, one should favor particles rendering square-like platelets as waxy and wheat starches. Normal maize SNC seems to contain both round- and square-like particles. Potato and high amylose SNC on the contrary presented disk-like platelets. Rheological properties of SNC suspensions from different starches have also been compared for the first time. The differences in viscosity can be quite important and will strongly help the selection of the best source depending on application.

Acknowledgments The research leading to these results has received funding from the European Community's Seventh Framework Programme (FP7/2007–2013) under grant agreement no. 207810.

References

- Angellier H (2005) Nanocristaux d'amidon de maïs cireux pour applications composites. PhD thesis, University Joseph Fourier, Grenoble, France
- Angellier H, Choïnard L, Molina-Boisseau S, Ozil P, Dufresne A (2004) Optimization of the preparation of aqueous suspensions of waxy maize starch nanocrystals using a response surface methodology. *Biomacromolecules* 5:1545–1551
- Angellier H, Molina-Boisseau S, Lebrun L, Dufresne A (2005) Processing and structural properties of waxy maize starch nanocrystals reinforced natural rubber. *Macromolecules* 38(9):3783–3792
- Angellier-Coussy H, Putaux J-L, Molina-Boisseau S, Dufresne A, Bertoft E, Perez S (2009) The molecular structure of waxy maize starch nanocrystals. *Carbohydr Res* 344(12):1558–1566
- Araki J, Wada M, Kuga S, Okano T (1999) Influence of surface charge on viscosity behavior of cellulose microcrystal suspension. *J Wood Sci* 45(3):258–261
- Bailey JM, Whelan WJ (1961) Physical properties of starch. I. Relationship between iodine stain and chain length. *J Biol Chem* 236(4):969–973
- Baker AA, Miles MJ, Helbert W (2001) Internal structure of the starch granule revealed by AFM. *Carbohydr Res* 330(2):249–256
- Battista OA (1975) *Microcrystal polymer science*. McGraw-Hill Book Company, New York, p 138

- Blanshard JMV (1987) Starch granule structure and function: a physicochemical approach. In: Galliard T (ed) *Starch: properties and potentials*, vol 13. Critical reports on applied chemistry. Society of Chemical Industry, London, pp 16–54
- Bras J, Viet D, Bruzzese C, Dufresne A (2011) Correlation between stiffness of sheets prepared from cellulose whiskers and nanoparticles dimensions. *Carbohydr Polym* 84(1):211–215
- Celzard A, McRae E, Deleuze C, Dufort M, Furdin G, Marêché JF (1996) Critical concentration in percolating systems containing a high-aspect-ratio filler. *Phys Rev B* 53(10):6209–6214
- Cheatham NWH, Tao L (1998) Variation in crystalline type with amylose content in maize starch granules: an X-ray powder diffraction study. *Carbohydr Polym* 36(4):277–284
- Chen G, Wei M, Chen J, Huang J, Dufresne A, Chang PR (2008) Simultaneous reinforcing and toughening: new nanocomposites of waterborne polyurethane filled with low loading level of starch nanocrystals. *Polymer* 49(7):1860–1870
- Dufresne A (2007) Polymer nanocomposites from biological sources. In: Bertolini AC (ed) *Biopolymers technology*. Cultura Academica, Sao Paulo, pp 59–83
- Dufresne A, Cavaillé J-Y (1998) Clustering and percolation effects in microcrystalline starch-reinforced thermoplastic. *J Polym Sci B* 36(12):2211–2224
- Dufresne A, Cavaillé JY, Helbert W (1996) New nanocomposite materials: microcrystalline starch reinforced thermoplastic. *Macromolecules* 29(23):7624–7626
- Duprat F, Gallant DJ, Guilbot A, Mercier C, Robin JP (1980) L'amidon. In: Monties B (ed) *Les Polymères Végétaux*. Polymères pariétaux et alimentaires non azotés. Gauthier Villars, Paris, pp 176–231
- Gallant DJ, Bouchet B, Baldwin PM (1997) Microscopy of starch: evidence of a new level of granule organization. *Carbohydr Polym* 32(3–4):177–191
- Gérard C, Planchot V, Colonna P, Bertoft E (2000) Relationship between branching density and crystalline structure of A- and B-type maize mutant starches. *Carbohydr Res* 326(2):130–144
- Imberty A, Perez S (1988) A revisit to the three-dimensional structure of B-type starch. *Biopolymers* 27(8):1205–1221
- Imberty A, Chanzy H, Perez S, Buleon A, Tran V (1987) New three-dimensional structure for A-type starch. *Macromolecules* 20(10):2634–2636
- Jane J-L, Wong K-S, McPherson AE (1997) Branch-structure difference in starches of A- and B-type X-ray patterns revealed by their Naegeli dextrans. *Carbohydr Res* 300(3):219–227
- Kasemsuwan T, Jane J (1994) Location of amylose in normal starch granules. II. Locations of phosphodiesterase cross-linking revealed by phosphorus-31 nuclear magnetic resonance. *Cereal Chem* 71:282–287
- Knutson CA (2000) Evaluation of variations in amylose-iodine absorbance spectra. *Carbohydr Polym* 42(1):65–72
- Le Corre D, Bras J, Dufresne A (2010) Starch nanoparticles: a review. *Biomacromolecules* 11(5):1139–1153
- Li J, Kim J-K (2007) Percolation threshold of conducting polymer composites containing 3D randomly distributed graphite nanoplatelets. *Compos Sci Technol* 67(10):2114–2120
- Lin N, Huang J, Chang PR, Anderson DP, Yu J (2011) Preparation, modification and application of starch nanocrystals in nanomaterials: a review. *J Nanomater* 2011:1–13
- Lopez-Rubio A, Flanagan BM, Gilbert EP, Gidley MJ (2008) A novel approach for calculating starch crystallinity and its correlation with double helix content: a combined XRD and NMR study. *Biopolymers* 89(9):761–768
- Lu C, Mai Y-W (2005) Influence of aspect ratio on barrier properties of polymer-clay nanocomposites. *Phys Rev Lett* 95(8):088303
- McGrance SJ, Cornell HJ, Rix CJ (1998) A simple and rapid colorimetric method for the determination of amylose in starch products. *Starch/Stärke* 50(4):158–163
- Nara S, Komiya T (1983) Studies on the relationship between water-saturated state and crystallinity by the diffraction method for moistened potato starch. *Starch/Stärke* 35(12):407–410
- Oates CG (1997) Towards an understanding of starch granule structure and hydrolysis. *Trends Food Sci Technol* 8(11):375–382
- Perez S, Baldwin PM, Gallant DJ (2009) Structural features of starch granules I. In: BeMiller J, Whistler R (eds) *Starch: chemistry and technology*, 3rd edn. Food science and technology. Academic Press, New York, p 176
- Putaux JL, Molina-Boisseau S, Momaour T, Dufresne A (2003) Platelet nanocrystals resulting from the disruption of waxy maize starch granules by acid hydrolysis. *Biomacromolecules* 4(5):1198–1202
- Robin J-P (1976) Comportement du grain d'amidon à l'hydrolyse acide ménagée. *Etude Physico-Chimique et Enzymatique de la fraction insoluble*. Contribution à la connaissance de la structure de l'amylopectine. Université Pierre et Marie Curie de Paris, Nancy
- Shannon JC, Garwood DL, Boyer CD (2009) Genetic and physiology of starch development. In: BeMiller J, Whistler R (eds) *Starch: chemistry and technology*, 3rd edn. Food science and technology. Academic Press, New York, p 28
- Siró I, Plackett D (2010) Microfibrillated cellulose and new nanocomposite materials: a review. *Cellulose* 17(3):459–494
- Szymonska J, Krok F (2003) Potato starch granule nanostructure studied by high resolution non-contact AFM. *Int J Biol Macromol* 33(1–3):1–7
- Waigh TA, Gidley MJ, Komanshek BU, Donald AM (2000a) The phase transformations in starch during gelatinisation: a liquid crystalline approach. *Carbohydr Res* 328(2):165–176
- Waigh TA, Kato KL, Donald AM, Gidley MJ, Clarke CJ, Riekkel C (2000b) Side-chain liquid-crystalline model for starch. *Starch/Stärke* 52(12):450–460
- Whistler RL, BeMiller J (2009) *Starch: chemistry and technology*, 3rd edn. Academic Press, New York
- Whistler RL, BeMiller JN, Paschall EF (1967) *Starch: chemistry and technology*, vol 2, 2nd edn. Academic Press, New York
- Williams PC, Kuzina FD, Hlynka I (1970) A rapid colorimetric procedure for estimating the amylose content of starches and flours. *Cereal Chem* 47:411–421